Paper No.
04375

CORROSION2004

HIGH PRESSURE CO_2 CORROSION ELECTROCHEMISTRY AND THE EFFECT OF ACETIC ACID

Shihuai Wang, Keith George and Srdjan Nesic
Institute for Corrosion and Multiphase Technology
Ohio University, Athens, OH 45701

ABSTRACT

The carbon dioxide corrosion electrochemistry of mild steel has been studied in the presence of high CO_2 partial pressures and acetic acid (HAc). Potentiodynamic sweeps, linear polarization resistance (LPR) and weight loss (WL) experiments have been conducted to investigate the effects of flow velocity, CO_2 partial pressure, and acetic acid concentration on the corrosion rate of mild steel. Electrochemical impedance spectroscopy measurements have also been conducted to help elucidate the corrosion mechanisms under the test conditions.

Keywords: high pressure, CO_2 corrosion, electrochemistry, acetic acid, linear polarization resistance, electrochemical impedance spectroscopy

INTRODUCTION

Due to the high cost and poor repeatability, very little experimental work on CO_2 corrosion at high pressures and temperatures has been performed in large-scale flow facilities[1]. No systematic electrochemical studies at such conditions have ever been done to shed light on the corrosion mechanism using potentiodynamic sweeps and/or transient techniques such as EIS. As a result, there is a lack of reliable electrochemical data and little understanding of the mechanism of CO_2 corrosion at high pressure and temperature. Therefore most of the mechanistic and semi-empirical models presently used in industry for predicting CO_2 corrosion are based on low-pressure (typically glass cell) experiments and extrapolate to the high pressure and temperature conditions found in the field.

The present electrochemical study of CO_2 corrosion of mild steel at high CO_2 partial pressures and in the presence of HAc has been completed to fill in the gap and focuses on investigating the main parameters that affect the corrosion rate such as: flow velocity, CO_2 pressure and HAc concentration. Using the experimental data which were generated, an electrochemical model,[1,2] based predominantly on low-pressure glass cell work, has been tested and calibrated for corrosion rate prediction under these test conditions. The comparison between the electrochemical model prediction and experimental data is presented separately.[3] Furthermore, the experimental results have been also used to calibrate the

advanced mechanistic corrosion model[4,5,6] built into the new 2003 version of Ohio University Corrosion in Multiphase Flow V3.0 software package.[7]

EXPERIMENTAL SETUP AND PROCEDURE

The experiments were carried out under in a 0.106 m I.D. inclinable stainless steel multiphase flow loop. A schematic sketch of the system is shown in Figure 1. To begin an experiment, the system was filled with 1515 L of de-ionized water containing 1% (mass) sodium chloride. The solution was de-aerated by purging CO_2 gas through the solution and flashing (for approximately 3 days) until the concentration of dissolved oxygen in the system was measured to be below 20 ppb. Experiments were conducted at three CO_2 partial pressures: 3 bar, 10 bar and 20 bar. The solution pH was maintained at 5.00 ± 0.05 using sodium bicarbonate and hydrochloric acid in all of the experimental work. For each CO_2 partial pressure, three water velocities of 0.2 m/s, 1 m/s, and 2 m/s were tested (single-phase flow) and the temperature of the test section was maintained at 60 ± 1°C. In selected experiments, at 10 bar CO_2 partial pressure, the effect of HAc was investigated, by varying the total HAc concentration from 0 to 1000 ppm.

The corrosion rate and mechanisms were studied using the electrochemical techniques of liner polarization resistance (LPR), potentiodynamic sweep and electrochemical impedance spectroscopy (EIS). Due to the configuration of the flow loop, two electrochemical probes could be inserted in the loop at the same time. This allowed for the measurement of a potentiodynamic sweep and an EIS scan to be conducted simultaneously and each sweep was done at least twice to ensure reproducibility of the results. LPR was conducted before and after every PS and EIS measurement. Weight loss (WL) measurements were also performed to compare with the electrochemical techniques.

Before each potentiodynamic sweep experiment, the electrode surface was polished with 400 and then 600 grit silicon carbide paper and washed with alcohol. This was done with extreme care as it was found that the condition of the surface could significantly affect the open circuit potential, which made any subsequent potentiodynamic sweeps problematic. Once the open circuit potential stabilized within 10 mV of the expected value, LPR measurements were conducted for 1-2 hours. This was followed by a cathodic sweep starting from the open corrosion potential to 500-650 mV below the open circuit potential. The electrode was then allowed to equilibrate until the open circuit potential was recovered (within 10 mV) which typically took 15 to 20 min. An anodic sweep was then conducted starting from the open corrosion potential and sweeping to 150-200 mV above. The scanning rate used in all cases was 0.2 mV/s. In the plots below all the potentials are referred to an arbitrary chosen reference potential.

The same polishing treatment (400 and then 600 grit silicon carbide paper) was performed before each EIS measurement was taken. LPR measurements were taken 1-2 hours after probe insertion and after the EIS measurements were taken. The EIS measurements were done by applying an oscillating potential ±5 mV to the working electrode at the open corrosion potential by using the frequency range 10 kHz - 1 mHz.

RESULTS AND DISCUSSION – CO_2 CORROSION WITHOUT HAc

The Effect of Velocity

Measurements at 3 bar CO_2

The effect of velocity at a partial pressure of 3 bar CO_2 on the potentiodynamic sweeps is shown in Figure 2. It is evident that the anodic reaction is unaffected by the velocity change and is under charge transfer control. The cathodic reaction is limiting current controlled and is only slightly affected by the velocity. This can be explained by the known fact that the carbonic acid contribution to the limiting current is governed by the slow kinetics of CO_2 hydration rather then by mass transport and is therefore not affected by the change in flow velocity. Due to the dominance of carbonic acid in the solution at these conditions (large CO_2 partial pressure, high pH), the effect of velocity on the limiting current is small.

The effect of liquid velocity on the Nyquist impedance plots is shown in Figure 3. Since the semi-circles at moderate frequencies and the inductive loops at low frequencies are overlapping for different velocities, this is further evidence that the effect of velocity on the corrosion mechanism is small under these conditions. More complex analysis and modeling of EIS spectra aiming to further elucidate the CO_2 corrosion mechanism is under the way.

Measurements at 10 bar CO_2

The effect of velocity at a partial pressure of 10 bar CO_2 on the potentiodynamic sweeps is shown in Figure 4. It is evident that the anodic reaction is again unaffected by the velocity change being charge transfer controlled. The cathodic reaction is fully limiting current controlled and was also unaffected by the velocity.

The effect of velocity on the Nyquist impedance plot at 10 bar CO_2 is shown in Figure 5. It also shows that the corrosion mechanism at 10 bar CO_2 is unaffected by the velocity.

Measurements at 20 bar CO_2

The effect of velocity at a partial pressure of 20 bar CO_2 on the potentiodynamic sweeps is shown in Figure 6. The anodic reaction is again unaffected by the velocity change. The cathodic limiting currents seem to show a slight velocity dependence which was unexpected since the limiting currents measured at 10 bar were unaffected by velocity (see Figure 4).

The effect of velocity on the Nyquist impedance plot at 20 bar CO_2 is shown in Figure 7. The effect of velocity seen there is small but repeatable.

The Effect of CO_2 Partial Pressure

The same data can be presented differently to study the effect of CO_2 partial pressure. Potentiodynamic sweeps at 0.2 m/s are shown in Figure 8 for various CO_2 partial pressures. It is evident that the anodic reaction was unaffected by the change in CO_2 partial pressure while the cathodic limiting current was strongly influenced. With an increase of CO_2 partial pressure, the limiting current is shifted to higher current densities due to the dominant effect of carbonic acid. Similar findings were found at 1.0 and 2.0 m/s and are shown in Figure 9 and Figure 10.

The effects of CO_2 partial pressures on the Nyquist impedance plots at 0.2 m/s, 1 m/s, 2 m/s liquid velocities are shown in Figure 11, Figure 12 and Figure 13 respectively. For each liquid velocity, the corrosion rates were obviously altered by the CO_2 partial pressure as the "size" of the semicircle changed. However, CO_2 partial pressure imparted little change in the shape of the impedance plot, suggesting a similar corrosion mechanism.

Weight Loss Experiments

The comparison between the experimental data (LPR and WL) at a partial pressure of 3 bar CO_2 is shown in Figure 14. The average value of any given data set is presented along with the error bars representing the maximum and minimum experimental values. The number of experimental data points used to calculate the average is given above the error bar. It is evident that the experimental LPR and weight loss measurements are in good agreement. It is also evident that slight velocity dependence can be seen in the corrosion rates, which was also present in the potentiodynamic sweeps (see Figure 2).

The comparison between the experimental data at 10 and 20 bar is shown in Figures 15 and 16. Again it is evident that the experimental LPR and WL measurements are in agreement. At 10 bar CO_2, the LPR and WL data show no velocity dependence, which can also be found from the potentiodynamic sweeps (see Figure 4). At 20 bar CO_2, the LPR and WL data indicate a slight velocity dependence and which was also found in the potentiodynamic sweep measurements (see Figure 5).

RESULTS AND DISCUSSION – CO_2 CORROSION WITH HAc

The Effect of HAc Concentration

The effect of adding HAc, to 100 ppm, on the potentiodynamic sweeps is shown in Figure 17. It is worth noting that all concentrations of HAc designate the amount of HAc added to the system and not the undissociated concentration after the addition and pH adjustment to pH 5. As expected, the cathodic limiting current is shifted to higher current densities with an increase in HAc concentration. The anodic curve is virtually unaffected by the addition of HAc. It is worth noting that no retardation in the anodic potentiodynamic sweep is seen with the addition of HAc that has been reported to occur at room temperatures and in glass cells[2].

A further increase in the HAc concentration to 1000 ppm HAc is shown in Figure 18. It is evident that the anodic curve is again unaffected by the addition of the HAc. However, the cathodic curves were shifted to lower current densities. This was considered to be an experimental artifact and was ascribed to rapid film formation on the working electrode during the measurement process.

The effect of HAc concentration on the Nyquist impedance plot is shown in Figure 19. In all cases, with an increase in HAc concentration, the intercept of the real axis shifts slightly to lower values, which suggests a small increase in the corrosion rate. However, the shape of the impedance curve stayed virtually the same, suggesting an identical corrosion mechanism dominated by the high partial pressure of CO_2 i.e. high concentration of H_2CO_3 .

The Effect of Velocity

The effect of velocity at a 1000 ppm HAc concentration is shown in Figure 20. As expected, with an increase in velocity, the cathodic limiting currents increased due to increased HAc transport to the surface. The anodic curve was unaffected by the change in velocity.

Weight Loss Measurements

The comparison between the LPR and WL experimental data is shown in Figure 21. The average value of the measurement is shown and the error bars represent the maximum and minimum experimental values with the number of data points used to find the average shown above the error bars. First, it is evident that the LPR and WL experimental data at 0 ppm HAc are not in very good agreement. The corrosion rates from weight loss were conducted over 10-11 hours, while the LPR values are from the initial insertion of the probe before the electrochemical measurements were made. It is uncertain why the weight loss measurements would so much larger than the LPR measurements, which were performed on freshly polished steel surfaces. When 10 ppm HAc is added to the system, the weight loss data suggest little change in the corrosion rate. The LPR values at 10 ppm, however are in good agreement with the WL data.

An increase in the corrosion rate is evident when 100 ppm HAc is added to the system. It should be noted that the time for the weight loss experiment was shortened from 10 hours to 2, due to film formation. A 10 hour weight loss experiment was conducted and the corrosion rates from the 10 and 2 hour weight loss experiments and LPR values are shown in Figure 22. It is evident that the in order to compare the weight loss measurements with the LPR values, which were measured under film-free conditions, short exposure times must be used. It is worth noting that all of the 10 hour weight loss experiments (0, 10 and 100 ppm HAc) have approximately the same corrosion rate (see Figures 15 and 21).

An addition of 1000 ppm HAc increases the corrosion rate as measured by LPR. But, the corrosion rate, as measured by weight loss indicates the corrosion rate is similar in value to when 100 ppm HAc is present (see Figure 22). This suggests the corrosion rate is under charge transfer control which has also been seen in RCE systems containing HAc.

CONCLUSIONS

In the present electrochemical study of CO_2 corrosion of mild steel at high CO_2 partial pressure and in the presence of HAc, it was found that:

- The anodic reaction was charge transfer controlled and was unaffected by velocity, CO_2 partial pressure, or the addition of HAc.
- The cathodic reaction was limiting current controlled. In the absence of HAc, the cathodic limiting current was almost unaffected by velocity, suggesting the slow CO_2 hydration as the rate determining step. The presence of HAc increased the limiting current and made it more velocity sensitive due to a mass transfer controlled mechanism.

ACKNOWLEDGEMENTS

The authors would like to acknowledge the contribution of the consortium of companies whose continuous financial support and technical guidance led to the development of the published work. They are BP, ConocoPhillips, ENI, Petrobras, Saudi Aramco, Shell, Total, Champion Technologies, Clariant, MI Technologies and Nalco. The authors also wish to thank Dr. Frederic Vitse for helping with troubleshooting at the beginning of the project.

REFERNCES

1. A. Dugstad, L. Lunde, and K. Videm, "Parametric Study of CO_2 Corrosion of Carbon Steel," Corrosion/1994, paper no.14, (Houston, TX: NACE International, 1994).
2. K. George, "Electrochemical Investigation of Carbon Dioxide Corrosion of Mild Steel in the Presence of Acetic Acid", Master's Thesis, Ohio University, 2003.
3. K. George, S. Wang, and S. Nesic, "Electrochemical and Corrosion Modeling of CO_2 Corrosion of Mild Steel in the Presence of High Partial Pressures of CO_2 and Acetic Acid", Corrosion/2004, paper no.04379, (New Orleans, LA: NACE Internation, 2004).
4. 4. S. Nesic, M. Nordsveen, R. Nyborg, and A. Stangeland, "A Mechanistic Model for CO2 Corrosion with Protective Iron Carbonate Films", Corrosion/2001, paper no.40, (Houston, TX: NACE International, 2001).
5. M. Nordsveen, S. Nesic, R. Nyborg, and A. Stangeland, Corrosion, 59, no. 5, (2003): p. 443.
6. S. Nesic, M. Nordsveen, R. Nyborg, and A. Stangeland, Corrosion, 59, no. 6, (2003): p. 489.
7. Nesic, S. Wang, J. Cai, Y. Xiao, "An integrated CO_2 corrosion/multiphase flow model", Corrosion/2004, paper no. 04626, (New Orleans, LA: NACE International, 2004).

TABLE 1. Experiment conditions

Test solution	Water + 1 mass % NaCl
CO_2 partial pressure	3, 10, 20 bar
Temperature	60 °C
pH	5
Flow velocity (single-phase flow)	0.2, 1, 2 m/s
HAc concentration*	0, 10, 100, 1000 ppm
Corrosion measurement techniques	Potentiodynamic sweep
	C1018 weight loss coupons (WL)
	Linear Polarization Resistance (LPR)
	Electrochemical Impedance Spectroscopy (EIS)

* HAc concentration means the total HAc which includes the undissociated HAc and Ac^-.

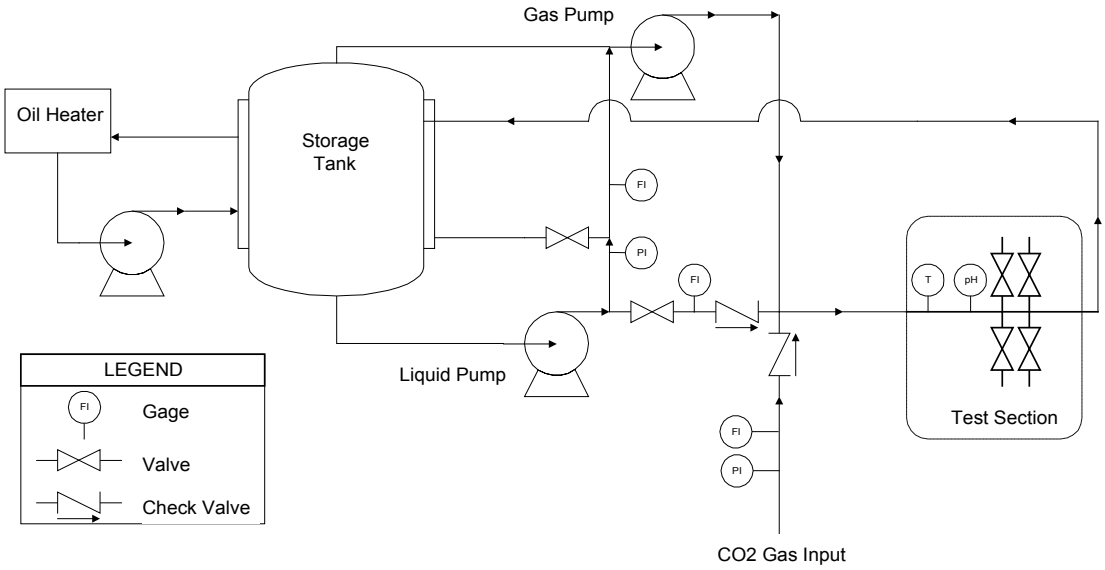

FIGURE 1. A schematic sketch of the test loop

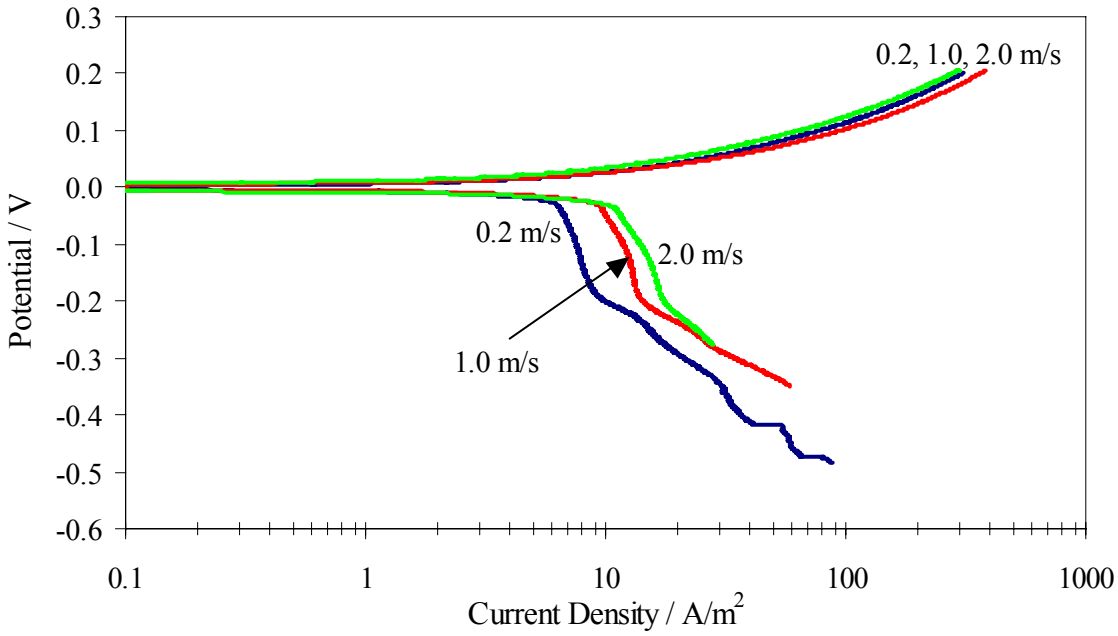

FIGURE 2. The effect of liquid velocity on the potentiodynamic sweeps at 3 bar CO_2 partial pressure (0.2-2.0 m/s, 60°C, pH 5).

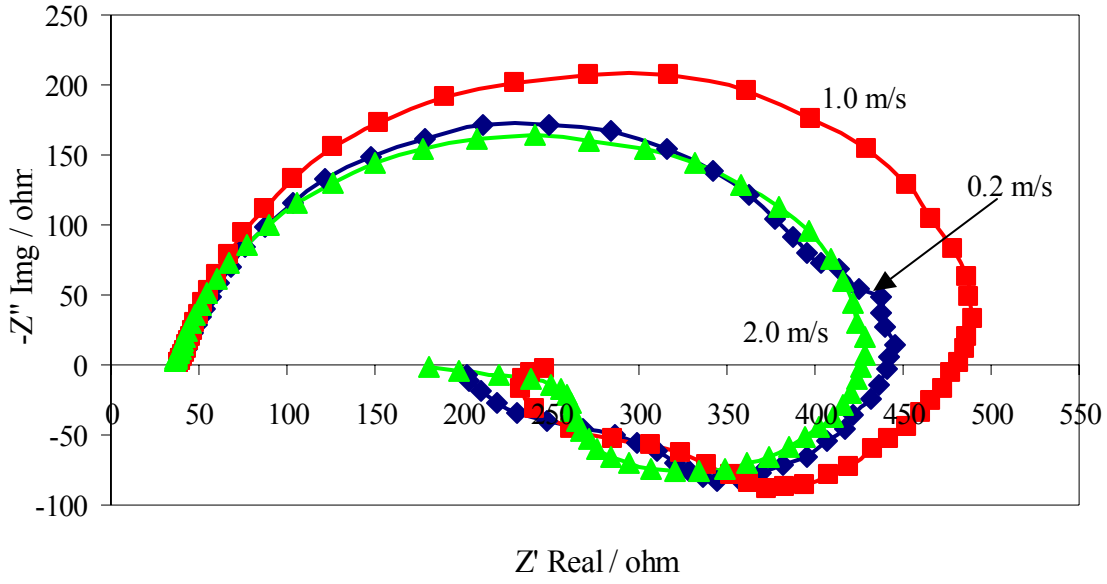

FIGURE 3. The effect of liquid velocity on the Nyquist impedance plots at 3 bar CO_2 partial pressure (0.2-2.0 m/s, 60°C, pH 5).

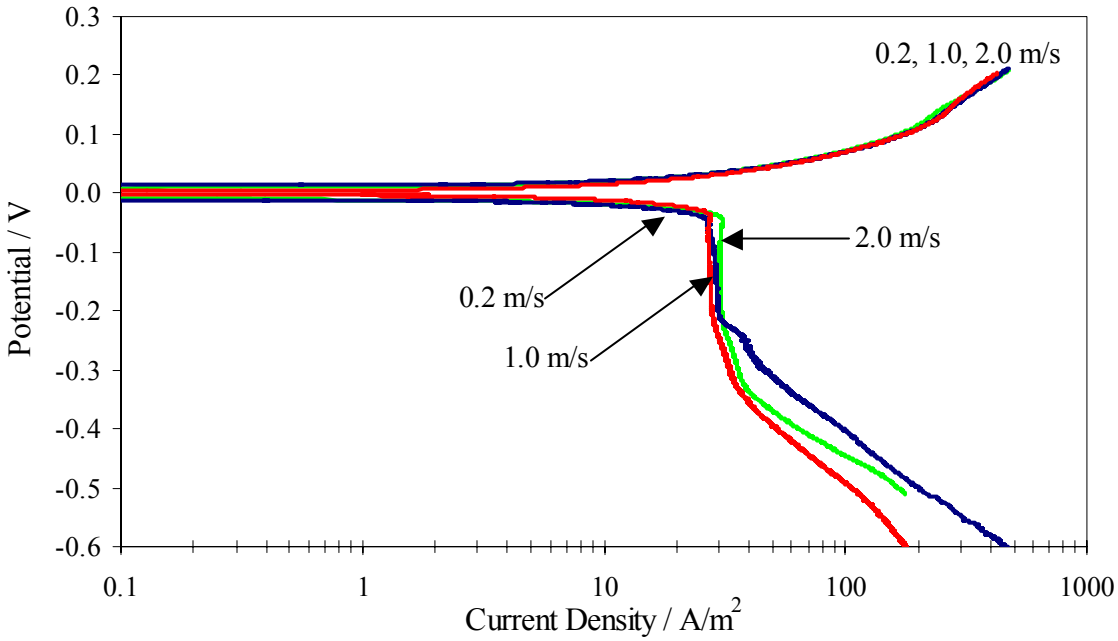

FIGURE 4. The effect of liquid velocity on the potentiodynamic sweeps at 10 bar CO2 partial pressure (0.2-2.0 m/s, 60°C, pH 5).

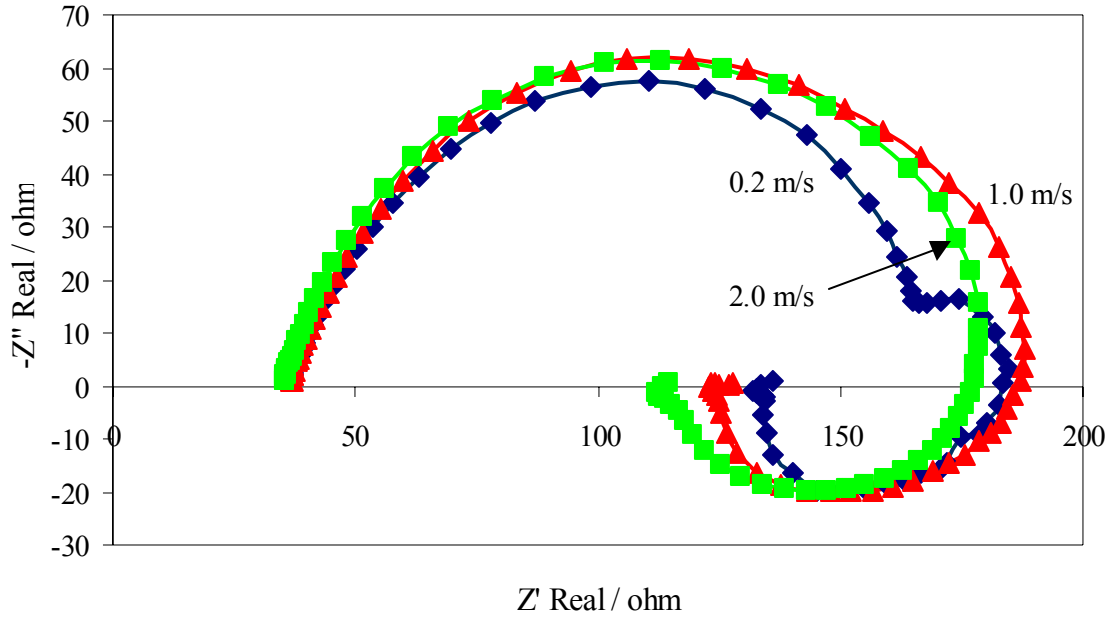

FIGURE 5. The effect of liquid velocity on the Nyquist impedance plots at 10 bar CO2 partial pressure (0.2-2.0 m/s, 60°C, pH 5).

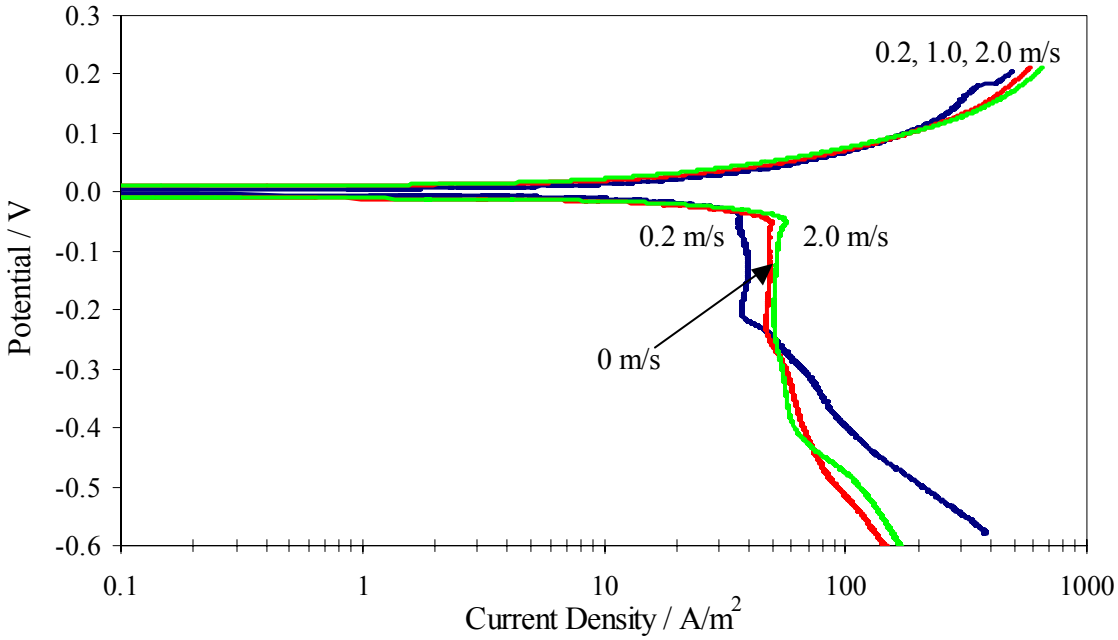

FIGURE 6. The effect of liquid velocity on the potentiodynamic sweeps at 20 bar CO_2 partial pressure (0.2-2.0 m/s, 60°C, pH 5).

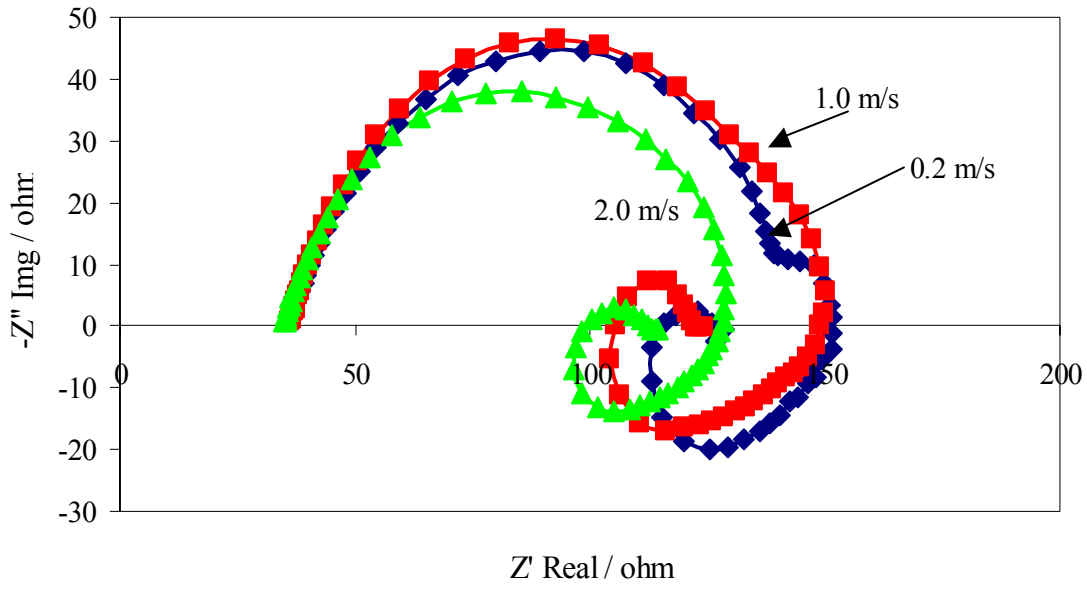

FIGURE 7. The effect of liquid velocity on the Nyquist impedance plots at 20 bar CO_2 partial pressure (0.2-2.0 m/s, 60°C, pH 5).

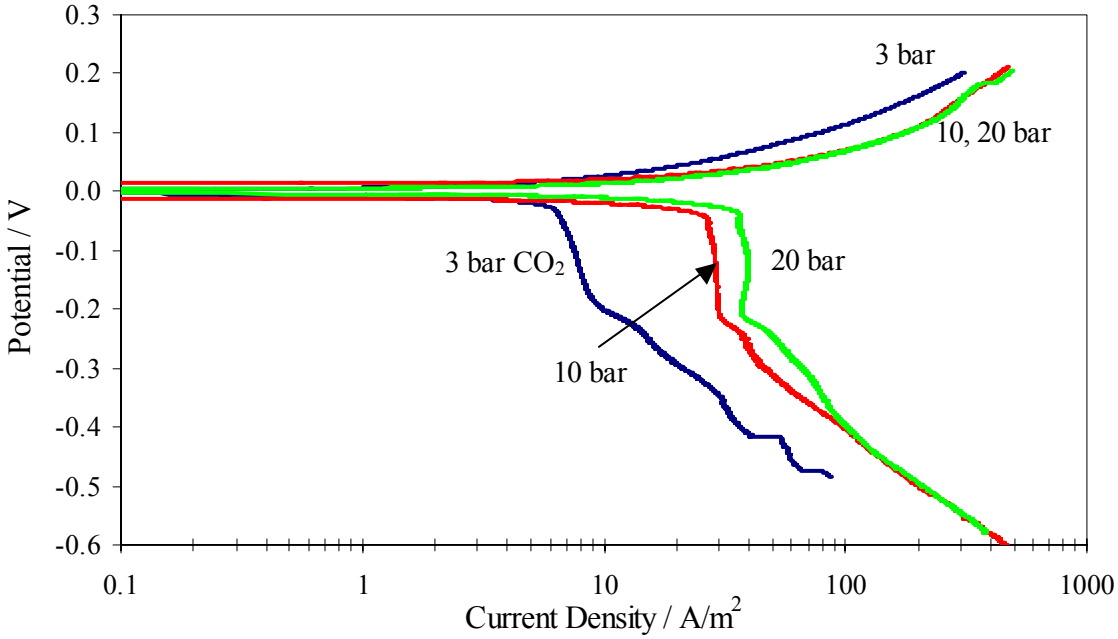

FIGURE 8. The effect of CO_2 partial pressure on the potentiodynamic sweeps at 0.2 m/s (3-20 bar CO_2, 60°C, pH 5).

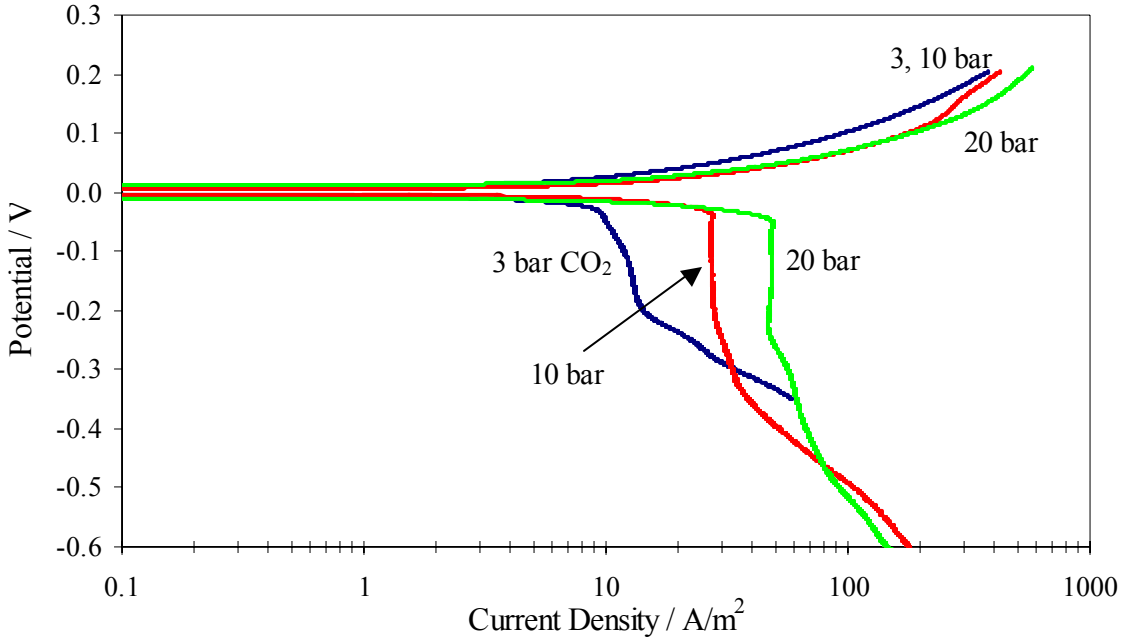

FIGURE 9. The effect of CO_2 partial pressure on the potentiodynamic sweeps at 1.0 m/s (3-20 bar CO_2, 60°C, pH 5).

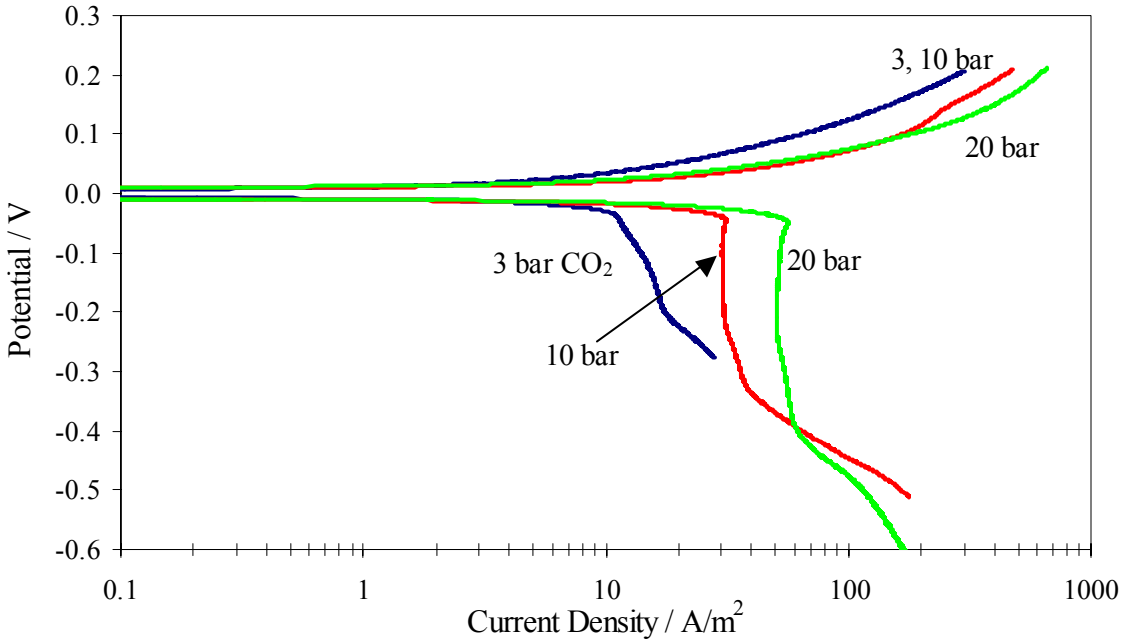

FIGURE 10. The effect of CO_2 partial pressure on the potentiodynamic sweeps at 2.0 m/s (3-20 bar CO_2, 60°C, pH 5).

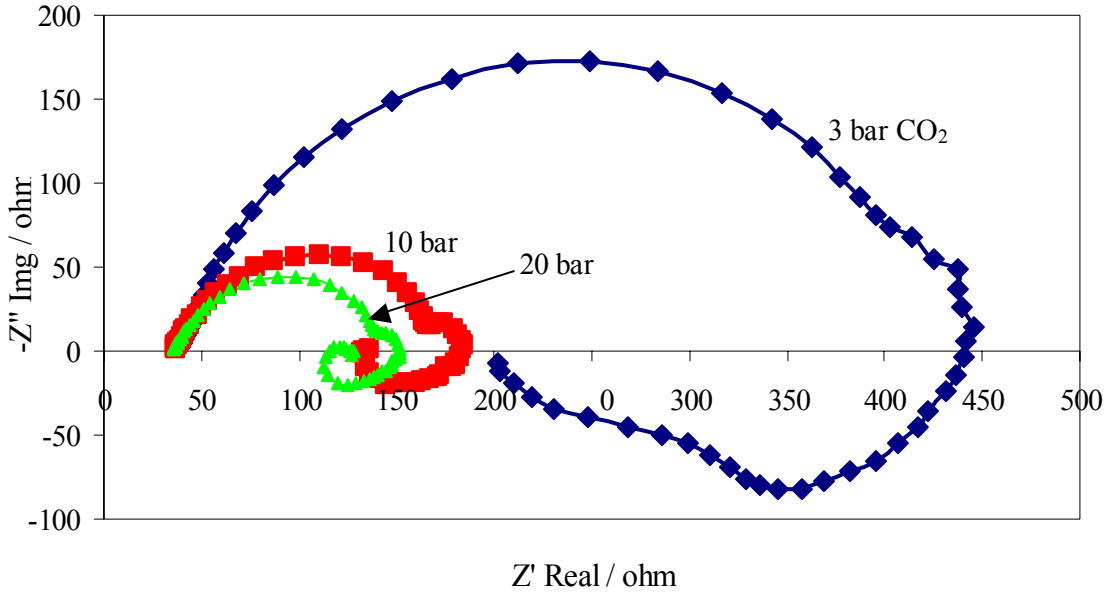

FIGURE 11. The effect of partial pressure of CO_2 on the Nyquist impedance plots at 0.2 m/s liquid velocity (3-20 bar, 60°C, pH 5).

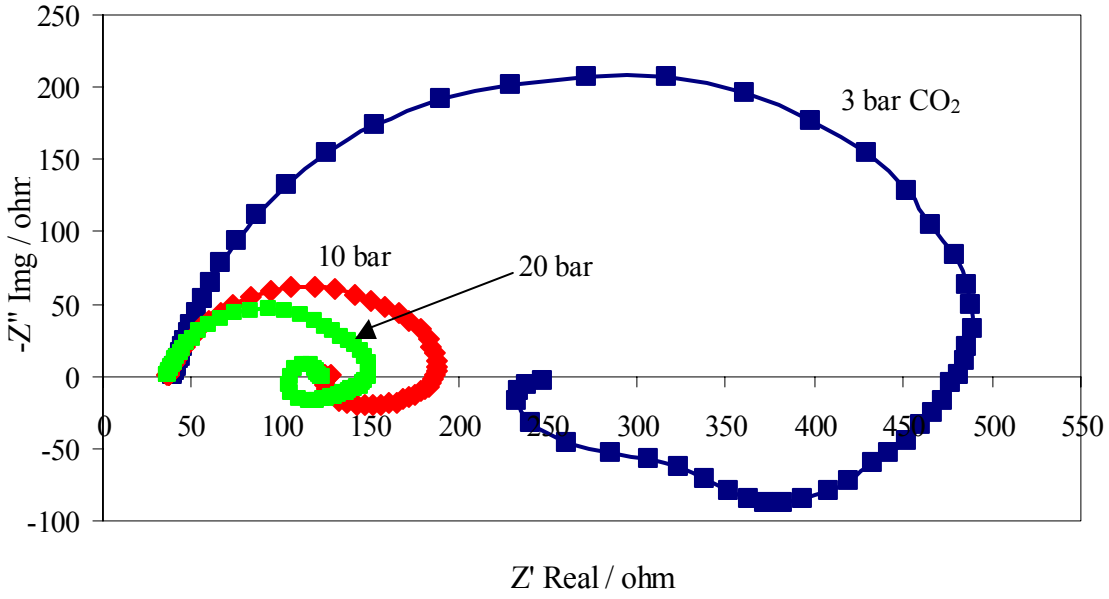

FIGURE 12. The effect of partial pressure of CO_2 on the Nyquist impedance plots at 1.0 m/s liquid velocity (3-20 bar, 60°C, pH 5).

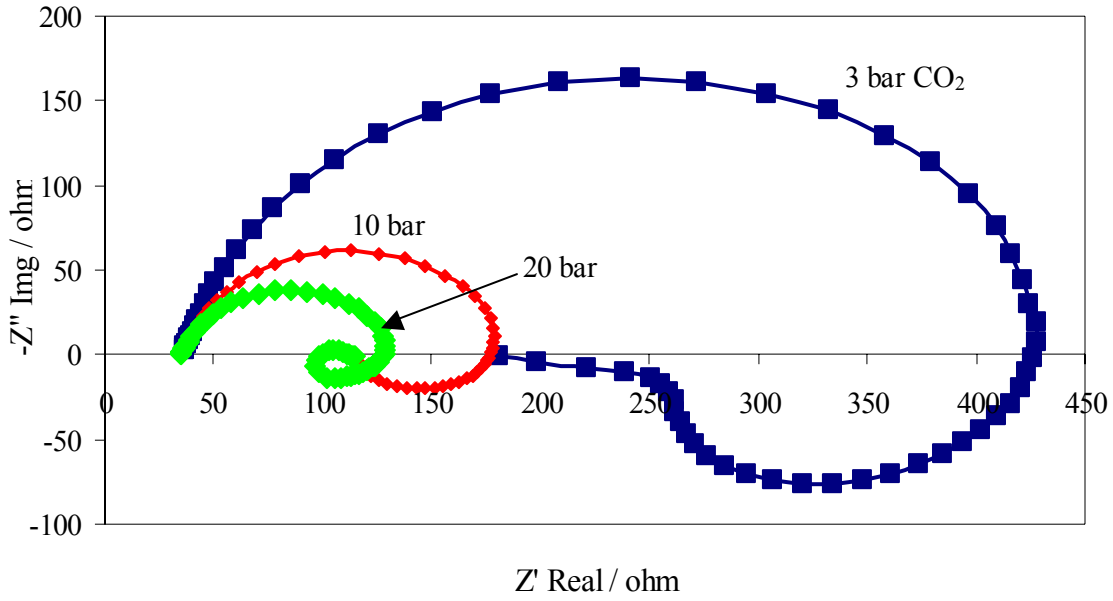

FIGURE 13. The effect of partial pressure of CO_2 on the Nyquist impedance plots at 2.0 m/s liquid velocity (3-20 bar, 60°C, pH 5).

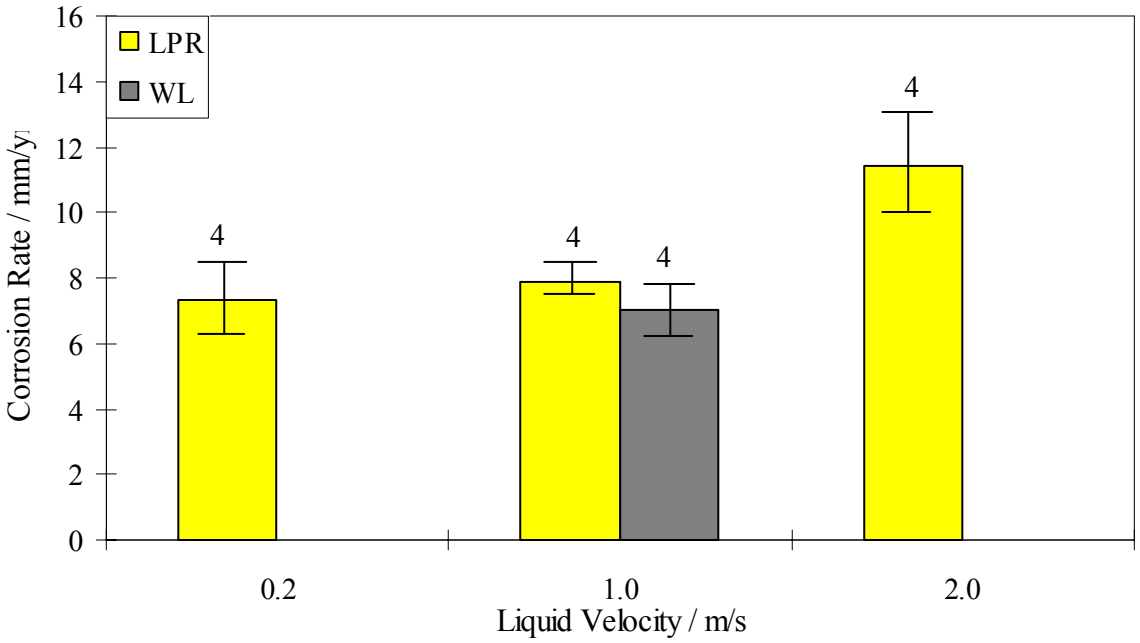

FIGURE 14. Comparison between the experimental LPR and weight loss data at 3 bar CO_2 partial pressure at 0.2, 1.0 and 2.0 m/s (60°C, pH 5,). Error bars represent maximum and minimum experimental values.

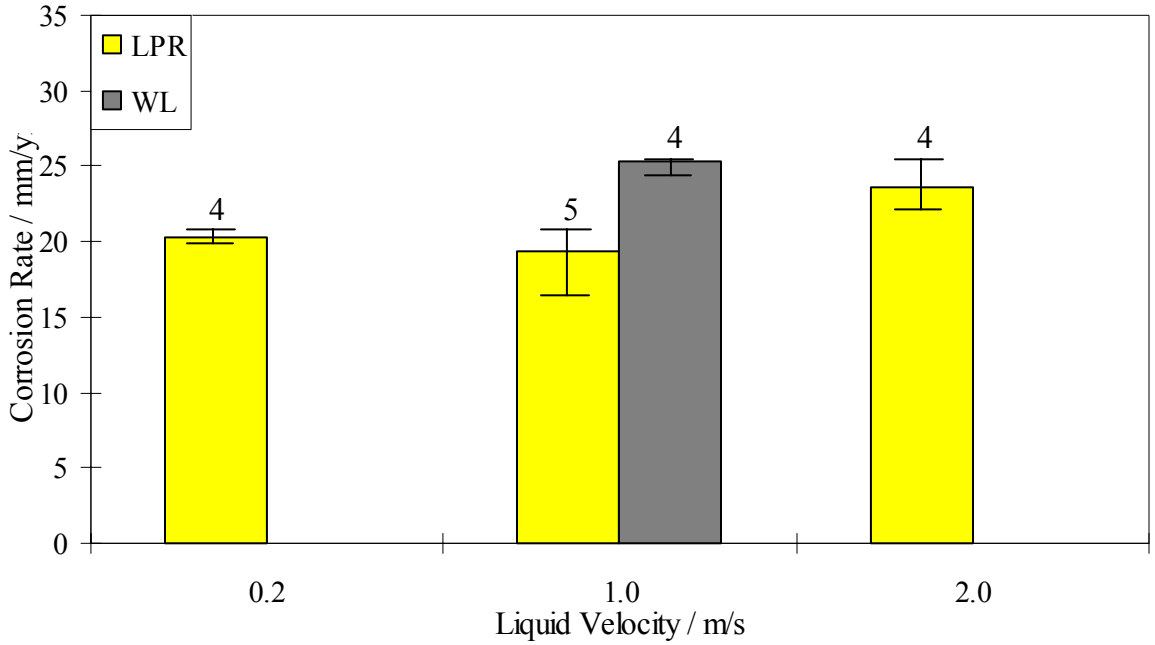

FIGURE 15. Comparison between the experimental LPR and weight loss data at 10 bar CO_2 partial pressure at 0.2, 1.0 and 2.0 m/s (60°C, pH 5,). Error bars represent maximum and minimum experimental values.

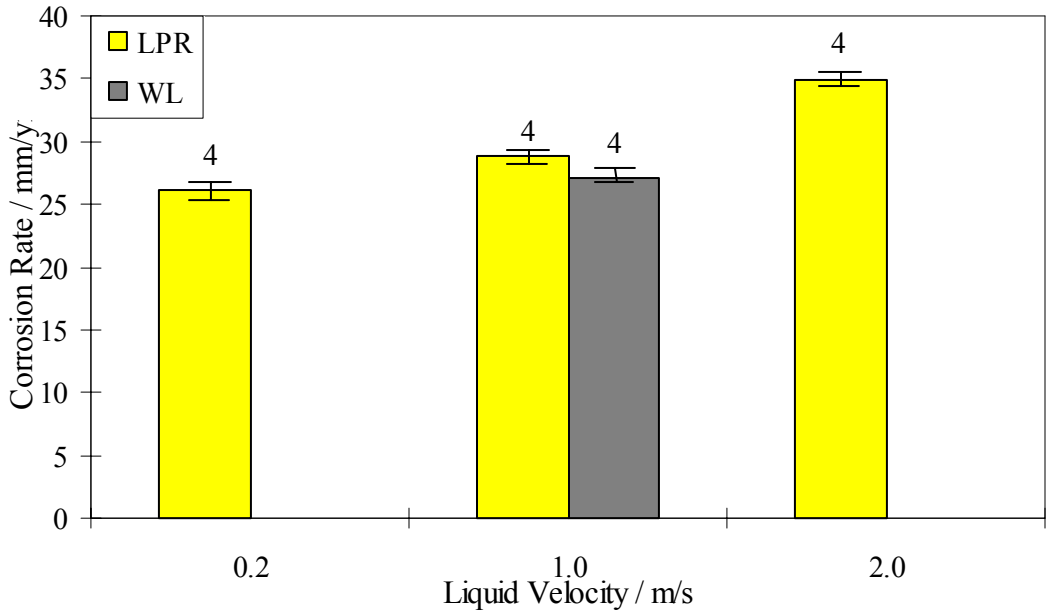

FIGURE 16. Comparison between the experimental LPR and weight loss data at 20 bar CO_2 partial pressure at 0.2, 1.0 and 2.0 m/s (60°C, pH 5,). Error bars represent maximum and minimum experimental values.

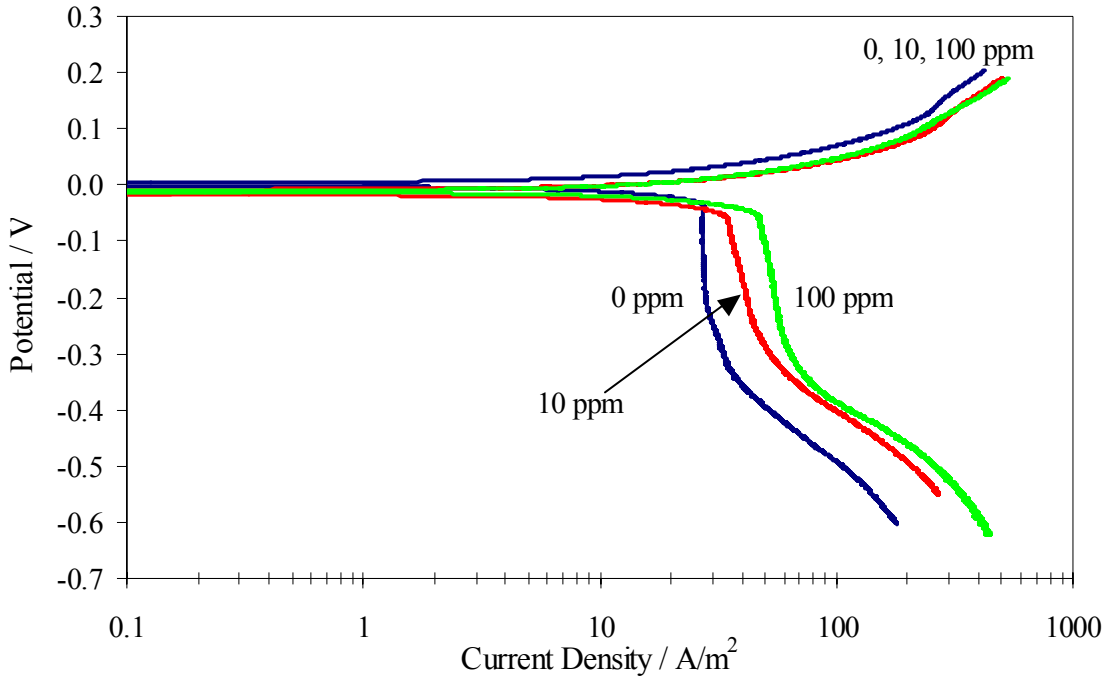

FIGURE 17. The effect of increasing HAc concentration on the potentiodynamic sweeps at a liquid velocity of 1 m/s (0-100 ppm HAc, 60°C, pH 5).

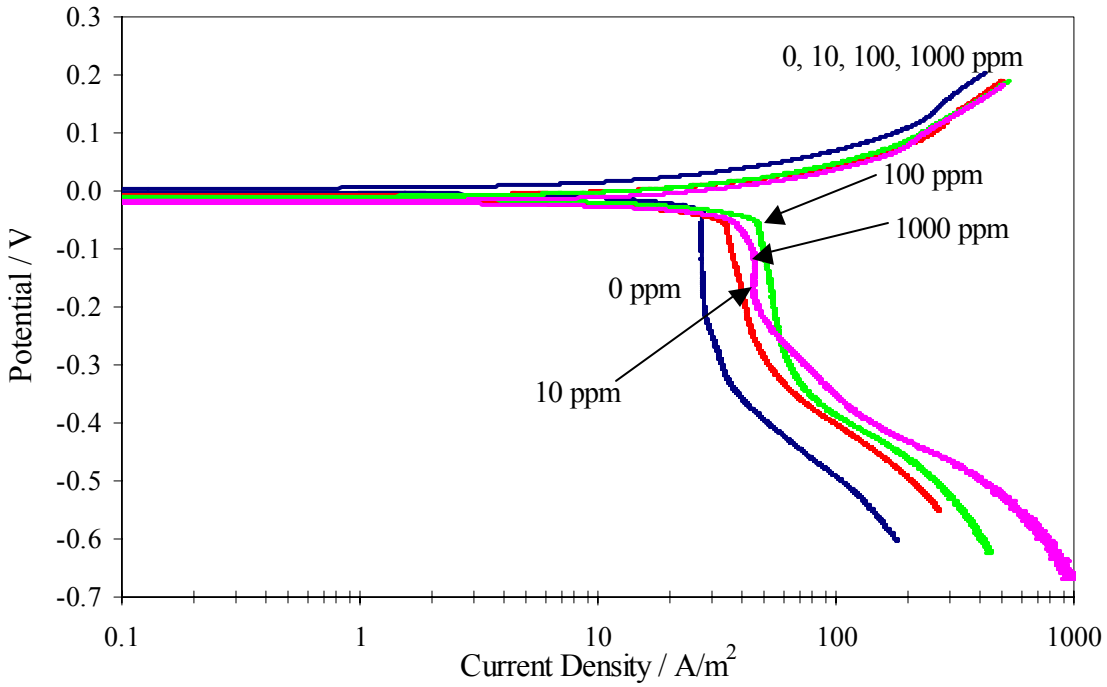

FIGURE 18. The effect of increasing HAc concentration on the potentiodynamic sweeps at a liquid velocity of 1 m/s (0-1000 ppm HAc, 60°C, pH 5).

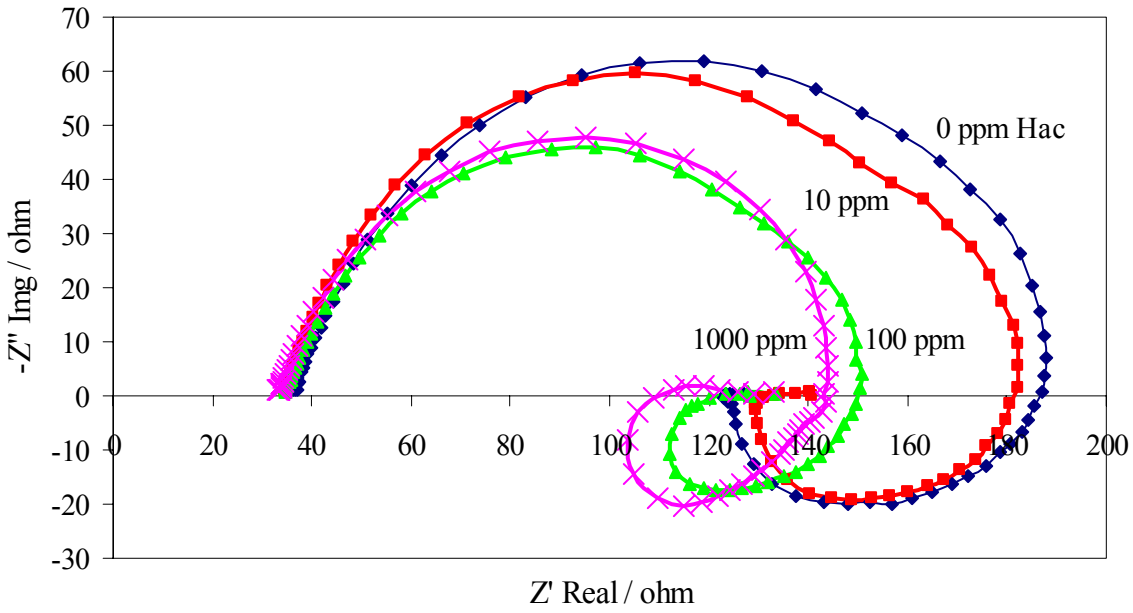

FIGURE 19. The effect of increasing HAc concentrations on the Nyquist impedance plots at a liquid velocity of 1 m/s (0-1000 ppm HAc, 60°C, pH 5).

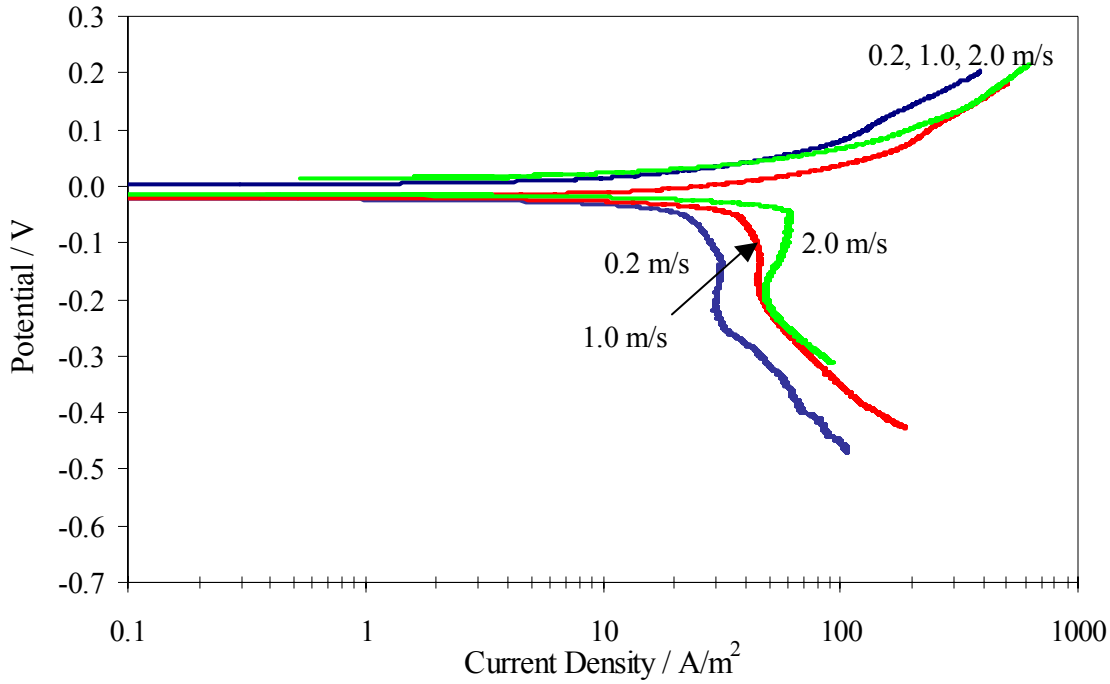

FIGURE 20. The effect of velocity on the potentiodynamic sweeps in solutions containing 1000 ppm HAc (0.2-2.0 m/s, 60°C, pH 5).

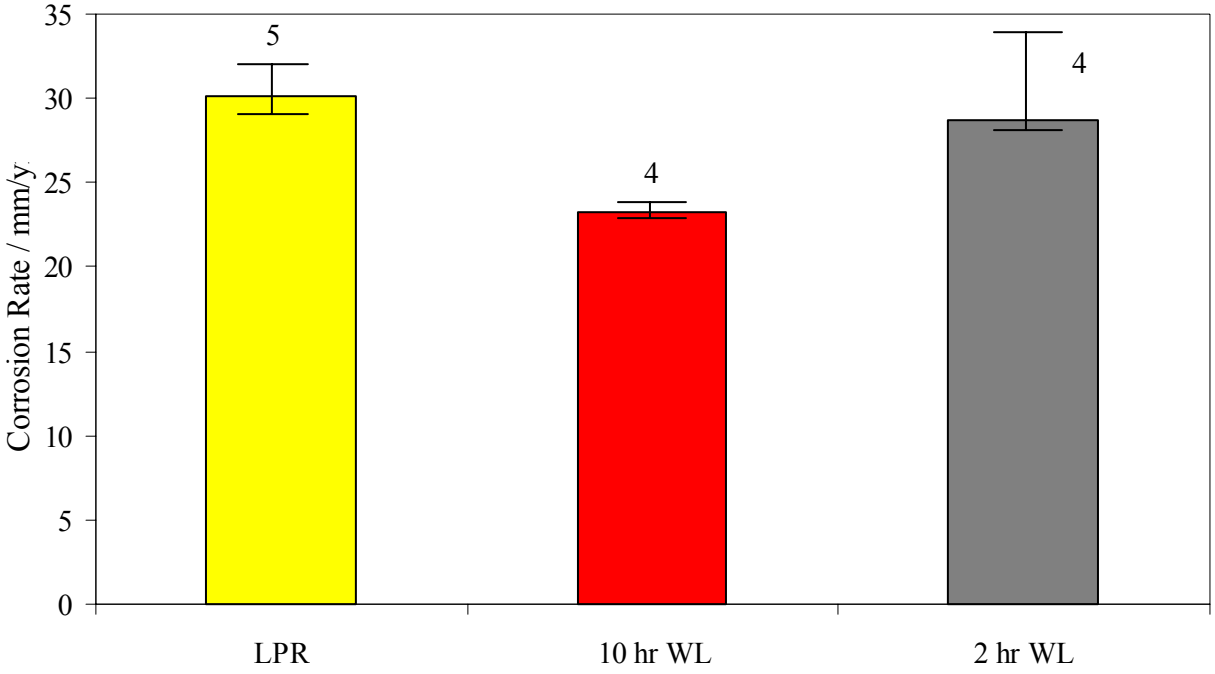

FIGURE 21. The comparison of the corrosion rates measured by weight loss with LPR measurements for different exposure times (100 ppm HAc, 60°C, pH 5, 10 bar CO_2, 1.0 m/s).

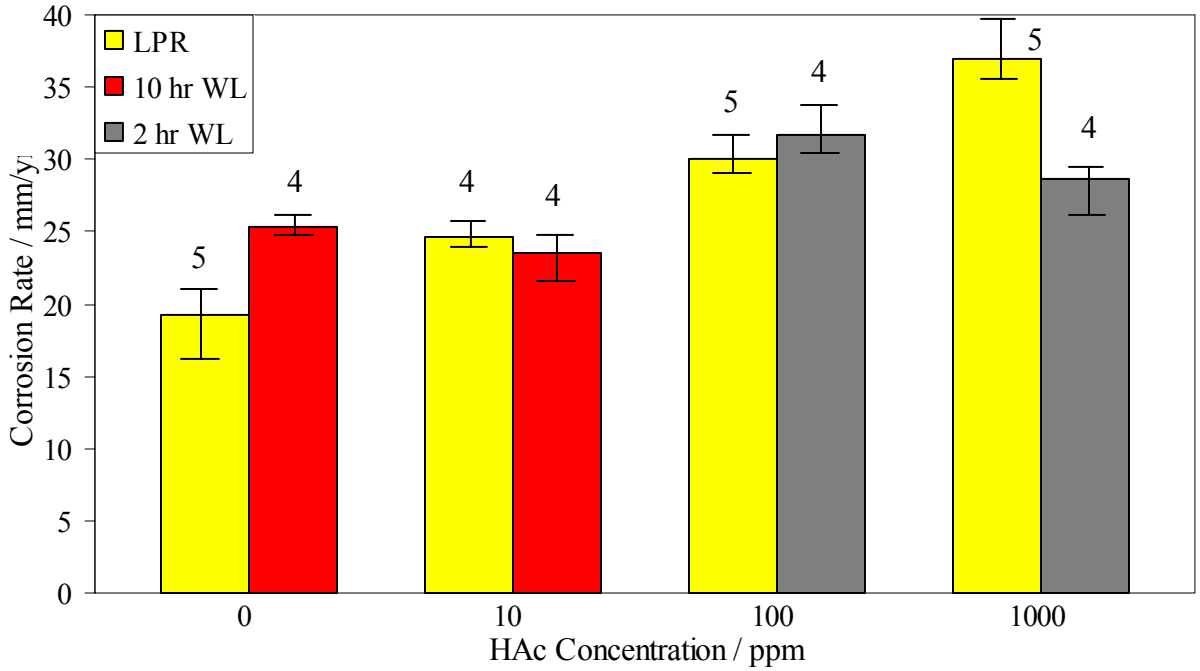

FIGURE 22. The effect of HAc concentration on the corrosion rate of mild steel measured using LPR and WL (0-1000 ppm HAc, 60°C, pH 5, 10 bar CO_2, 1.0 m/s). Error bars represent maximum and minimum experimental values.